JOURNAL OF SPACECRAFT AND ROCKETS
Vol. 31, No. 1, January–February 1994

Estimation of the Low-Earth-Orbit Debris Population and Distribution

Kyle T. Alfriend* and D. Laurie Lewis†
General Research Corporation, Vienna, Virginia 22182

In this paper an algorithm for estimating the low-Earth-orbit space object population and distribution from measurements taken by a vertical, staring narrow beam radar is developed and validated. The radar measures the altitude, inclination, and radar cross section of each object which passes through the beam. Validation of the algorithm is achieved by simulating the orbits of the objects in the North American Aerospace Defense Command (NORAD) data base, determining those which pass through a vertical staring radar and by estimating the population and distribution of the NORAD data base from the altitude, inclination, and radar cross section of those which pass through. The effects of the assumptions made in developing the algorithm and measurement errors are discussed. An estimate of the operational time of the radar needed to achieve a specified accuracy in the space object population is also developed.

Nomenclature

h = orbit altitude
I = orbit inclination
N = number of objects in population
N_{est} = estimated number of objects in population
r = orbit radius
T = orbit period
T_m = measurement time
α = Earth central angle subtended by radar
β = radar beamwidth
θ = latitude of radar
λ = expected rate of objects through radar beam
λ^* = measured rate of objects through radar beam

I. Introduction

CONCERN with the potential hazard to operational spacecraft caused by orbital debris has been increasing over the last few years as the number of space objects have increased and the realization of the hazard became evident. In particular, orbital debris poses a potential major hazard to Space Station Freedom (SSF). Table 1 summarizes the problem. Collision with an object smaller than 1 mm is not expected to cause catastrophic damage, but it can cause erosion. A collision with an object greater than 1 mm can potentially cause catastrophic damage. We are able to shield against collision with objects as large as 1 cm and this is planned for SSF. Since U.S. Space Command currently tracks objects greater than 10 cm, spacecraft can maneuver to avoid potential collisions with them, as the Space Shuttle has done on several occasions. The result is that objects in the range of 1–10 cm are a major threat to SSF and objects in the range of 0.1–10 cm are a major threat to unshielded spacecraft. Thus, there is a need to be able to track space objects as small as 1 cm. Studies addressing this problem are currently underway, but within the next several years we will not have the capability to track all of the objects in the 0.1–10 cm range. However, if we knew the number and distribution of objects down to 1 mm, we would at least be able to determine the probability of collision. The purpose of this paper is to develop an algorithm to determine the population and its distribution so that the probability of collision can be determined.

Some estimates of the total population have been made[1,2] from the Long Duration Exposure Facility (LDEF) and the Solar Max mission, but a much more definitive answer is needed. As a first step in determining the low-Earth-orbit debris environment, NASA has proposed a radar which would look vertically, count the number of objects passing through, and for each object obtain an estimate of radar cross section (RCS), altitude, inclination, and eccentricity. From these data an estimate of the population and distribution would be made. The GBR-X radar,[3] which was being developed at Kwajalein by the U.S. Army Strategic Defense Command, was a candidate, but this program has been canceled. Recently, some measurements have been made using the Haystack radar.[4] With Haystack, measurements have been made at three elevation angles: 10 deg, 20 deg, and 90 deg (vertical). Measurements were made at elevation angles other than the vertical because Haystack is at a latitude greater than the 28-deg inclined orbit of the Space Station and cannot measure the total environment of the Space Station looking vertically. With a 10-deg elevation looking due south, it can sample the 28-deg latitude region at the planned Space Station altitude.

In this paper, we develop and validate using simulation an algorithm for estimating the low-Earth-orbit space object population and distribution from measurements taken by a vertically looking radar such as Haystack or GBR-X. The development of the algorithm is presented in Sec. II and the validation in Sec. III. In Sec. IV potential error sources and their effect on the estimation are discussed.

II. Algorithm

In this section we develop the algorithm for estimating the low-Earth-orbit space object population and distribution from measurements of the altitude, inclination, and radar cross section (RCS) of a sample of the population. Errors in the estimates will be derived as a function of the sample size. A vertical-looking (bore sight = 90 deg) radar is used for the measurements. For each object which passes through the

Table 1 Object size, collision damage summary

Size, cm	Collision effect	Shielding	NORAD tracking
< 0.1	Possible erosion	Yes	No
0.1–1	Possible catastrophic damage	Yes	No
1–10	Possible catastrophic damage	Yes	No
> 0.1	Possible catastrophic damage	No	Yes

Received July 18, 1992; revision received Feb. 8, 1993; accepted for publication Feb. 9, 1993.

*Senior Scientist, 1900 Gallows Rd. Fellow AIAA.
†Engineer, 1900 Gallows Rd.

beam the range, inclination and RCS (within some accuracy) will be obtained. First, we state the assumptions, and then derive the algorithm. The effect of these assumptions on the estimation is discussed in Sec. IV.

Assumptions

1) All of the objects are in circular orbits at the altitude they pass through the radar. Since no accurate eccentricity and argument of perigee measurements are available, this assumption is necessary.

2) The right ascension and argument of latitude (true anomaly plus argument of perigee) of the low-earth-orbit space object population is uniformly distributed. An analysis of the NORAD data base validates this assumption.

3) There are no objects with inclinations approximately equal to the latitude of the sensor. The algorithm could be modified if there are objects in this category.

4) The problem of space objects passing through a radar beam can be modeled as a Poisson process. A Poisson process is characterized by the passage of objects whose times of passage are independent and possess a constant average rate of passage. Other problems characterized by a Poisson process are the random emissions from a filament and the passage of cars at a toll booth. For a constant average rate of objects through the beam, the parent population must be uniformly distributed in right ascension and argument of latitude (assumption 2).

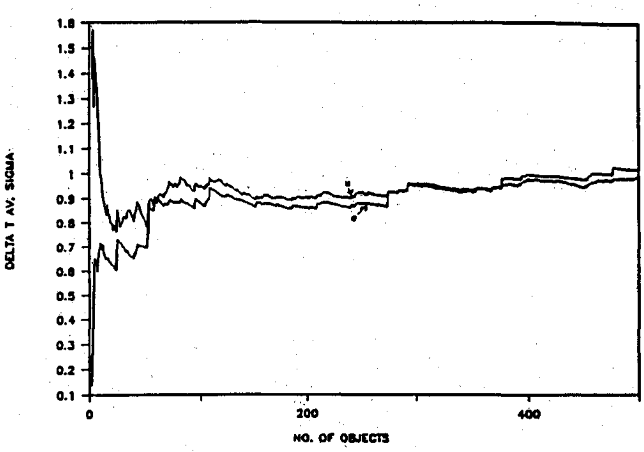

Fig. 1 Mean/standard deviation convergence, simulated Poisson process.

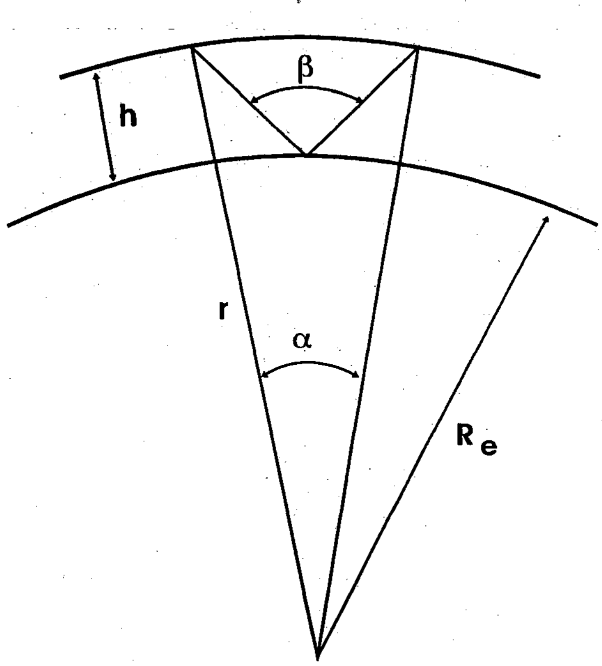

Fig. 2 Geometry of radar field of view, equatorial site.

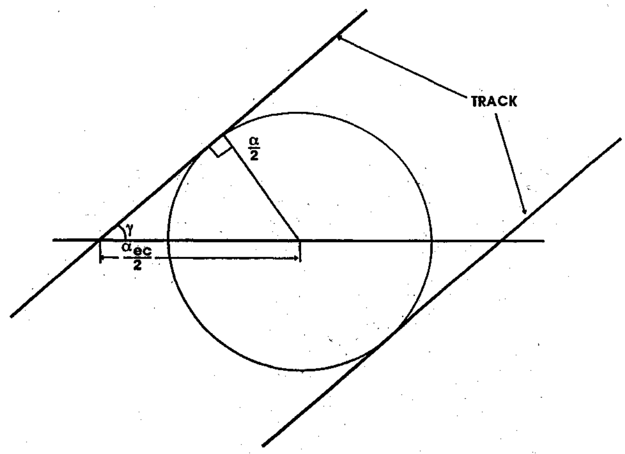

Fig. 3 Geometry of radar field of view, arbitrary latitude.

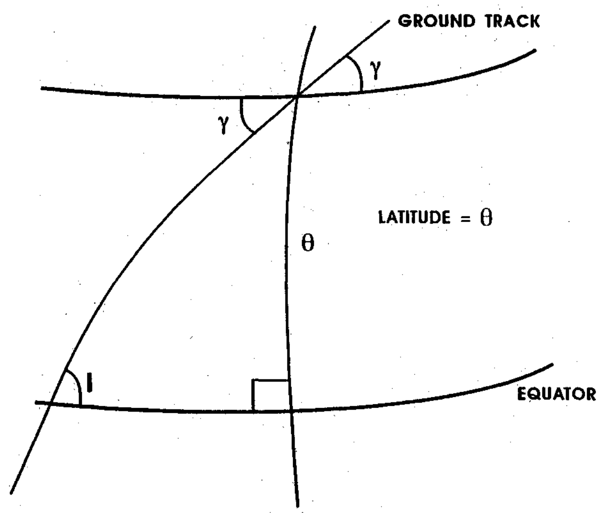

Fig. 4 Orbit geometry.

Two key properties of the Poisson process are as follows. First, the mean and standard deviation of a random process generated from the difference in times of passage of successive objects of a Poisson process are equal and equal to the inverse of the rate of objects. Figure 1 shows the convergence of the mean and standard deviation of a simulated Poisson process with an average rate of unity. The abscissa is equivalent to the number of objects which have passed through the radar beam. We can see that very good convergence is achieved after approximately 500 objects have passed through. We will see similar results for the space object population estimation. Second, the sum of independent Poisson processes is a Poisson process with a rate equal to the sum of the rates of the individual processes.

Algorithm

First consider a radar of beamwidth β which is located on the equator and a fence in the east-west direction as shown in Fig. 2. The Earth central angle α subtended by the radar at an altitude h (radius r) is $h\beta/r$ for small β. Consider N objects in circular orbits of the same altitude and inclination. Since each object crosses the equator, the rate of objects crossing is $2N/T$ where T is the orbital period. The rate of objects passing through the beam is just the product of this equatorial cross-

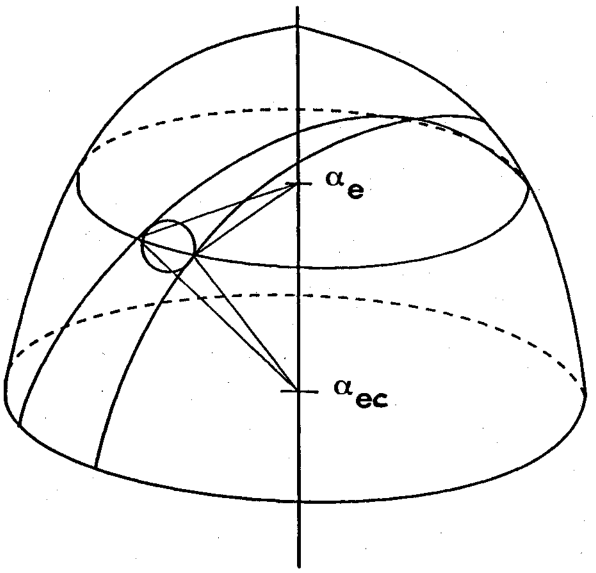

Fig. 5 Radar beamwidth, Earth central angle relation.

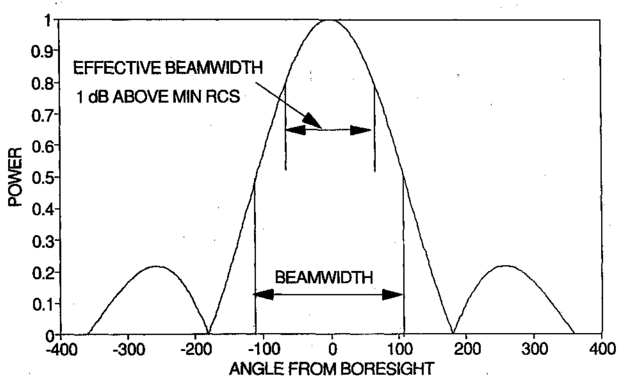

Fig. 6 Effective beamwidth.

ing rate and the ratio of the Earth central angle of the radar to the total angle of the equator, which is 2π, i.e.,

$$\text{rate} = \lambda = \frac{2N}{T}\frac{\alpha}{2\pi} = \frac{2N}{T}\frac{h\beta}{2\pi r} \tag{1}$$

To model the beam as a cone rather than a fence, which is located at a latitude θ, consider Fig. 3, which is a view looking down the bore sight of the radar of beamwidth β at altitude h. Also shown are the tracks of the satellites tangent to the cone. Because the radar is a cone, all of the objects crossing the latitude θ between these two tracks will pass through the radar. Thus, the radar has an effective beamwidth α_{ec} given by

$$\alpha_{ec} = \alpha/\sin\gamma \tag{2}$$

Referring to Fig. 4 and using spherical trigonometry

$$\cos\gamma = \cos I/\cos\theta \tag{3}$$

or

$$\sin\gamma = [\cos^2\theta - \cos^2 I]^{1/2}/\cos\theta \tag{4}$$

Following the same approach as with the fence, the rate of objects passing through the beam will be the product of the rate of objects crossing the latitude θ and the percentage the angle α_{ec} subtends the latitude line at latitude θ, or the percentage of right ascensions that will pass through the radar. From Fig. 5

$$\alpha_{ec} = \alpha_e \cos\theta \tag{5}$$

Substituting Eq. (5) into Eq. (4) and using Eq. (2) gives

$$\alpha_e = \alpha/[\cos^2\theta - \cos^2 I]^{1/2} \tag{6}$$

Replacing α with α_e in Eq. (1) and then substituting Eq. (6) gives

$$\lambda = \left(\frac{2N}{T}\right)\left(\frac{h\beta}{r}\right)\left(\frac{1}{2\pi[\cos^2\theta - \cos^2 I]^{1/2}}\right) \tag{7}$$

which is the average rate of objects passing through the radar beam of beamwidth β, located at latitude θ and looking vertically for a population of N objects at altitude h and inclination I. The beam angle β must be small, and the latitude θ must not be greater than or equal to the inclination of the objects. As $I \rightarrow \theta$, Eq. (7) is no longer valid and the algorithm has to be modified.

To expand this to the population which is large enough to be seen by the radar, we make use of the property that the sum of independent Poisson processes is a Poisson process with a rate equal to the sum of the individual rates. Therefore, for the entire population

$$\lambda = \frac{1}{\pi}\left[\sum_{i=1}^{N}\left(\frac{1}{T_i}\right)\left(\frac{h_i\beta_i}{r_i}\right)[\cos^2\theta - \cos^2 I_i]^{-1/2}\right] \tag{8}$$

Note that we are summing over the beamwidth β_i, that is, the beamwidth is different for each object. Consider Fig. 6 where the beamwidth is defined as the half-power (3 dB) point, and consider an object whose RCS is 2 dB greater than the minimum detectable RCS at the peak of the beam. The effective beamwidth for this object is the one shown because if the object passed through the beam further from the peak it would not be detected. This factor has to be considered or the number of objects will be underestimated. Data on the effective beamwidth have to be supplied or can be determined by assuming a $(\sin x/x)$ beam pattern.

Equation (8) represents the expected rate of objects for a given population. However, we want to estimate the population N from observations of a subset M of the population. Assuming we knew h, β, T, r, and I of every object in the population we could write

$$\lambda = \frac{N}{\pi}\left[\frac{1}{T}\frac{h\beta}{r}\frac{1}{\sqrt{\cos^2\theta - \cos^2 I}}\right]_{\substack{\text{tot}\\ \text{pop}\\ \text{avg}}} \tag{9}$$

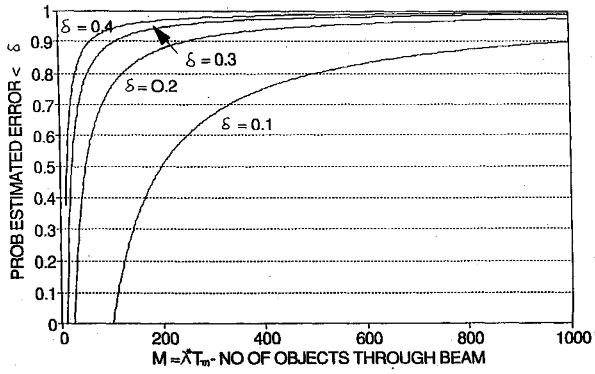

Fig. 7 Measurement time to achieve specified accuracy.

and solve for N. We will call the term in brackets [ ]tpa. We cannot calculate [ ]tpa, but we can estimate it from the observations, and, with the measured rate, estimate N. Essentially the quantity [ ]tpa is the transfer function of a filter that filters the space object population and allows some objects to be observed. To estimate the transfer function we apply the inverse filter to the observed data. Doing this gives

$$\left[\frac{1}{T}\frac{h\beta}{r}\frac{1}{\sqrt{\cos^2\theta - \cos^2 I}}\right]_{\text{avg}}^{\text{tot pop}} \approx \left[\frac{1}{M}\sum_{i=1}^{M}\frac{r_i T_i \sqrt{\cos^2\theta - \cos^2 I_i}}{h_i \beta_i}\right]^{-1} \tag{10}$$

where M is the number of observations or the number of objects which have passed through the beam. At this point, it is necessary to make the assumption that all of the objects are in circular orbits in order to compute T from the measurement data which provides an altitude but no information on eccentricity. The consequence of this assumption will be discussed later.

Knowing the total population average, we can solve for N_{est}, the estimated total population.

$$N_{\text{est}} = \lambda^* \pi \left[\frac{h\beta}{Tr\sqrt{\cos^2\theta - \cos^2 I}}\right]^{-1}_{\text{tot pop avg}} \tag{11}$$

where λ^* is the measured rate.

To estimate the true population distribution, this same procedure can be applied to only those observations falling into a particular altitude, inclination, or RCS range or bin. The resulting N_{est} will be the estimated number of objects in the total population in those bins.

Measurement Time

Analysis using the algorithm will determine the measurement time needed to provide the desired accuracy of the estimation. However, a quicker approach is desirable and available. We can apply Chebyshev's inequality[5] to the Poisson process.

Given a random variable x with mean μ, variance σ^2, density function $f(x)$, and a sample of size M from x, Chebyshev's inequality states that

$$Pr[|\bar{x} - \mu| < \epsilon] \geq 1 - \sigma^2/M\epsilon^2 \tag{12}$$

where x is the mean of the sample. The mean and variance of the distribution of sample means are given by

$$\mu_{\bar{x}} = \mu \tag{13}$$

$$\sigma_{\bar{x}}^2 = \sigma^2/M \tag{14}$$

Note that the inequality is independent of the density function $f(x)$.

Now apply this inequality to the space object population problem which is described by a Poisson process. N is the total population, N^* the estimated population, M the number of objects passing through the radar, and

$$\lambda^* = M/T_m \tag{15}$$

where T_m is the measurement time. For a Poisson process, $\sigma = \mu = \lambda^{-1}$. Let

$$\zeta = \epsilon/\mu \tag{16}$$

then

$$\sigma^2/M\epsilon^2 = (\lambda^* T_m \zeta^2)^{-1} \tag{17}$$

Dividing the term in brackets in Eq. (12) by μ leads to

$$Pr\left[\left|\frac{N}{N^*} - 1\right| < \zeta\right] \geq 1 - (\lambda^* T_m \zeta^2)^{-1} \tag{18}$$

To obtain a conservative estimate for T_m, we can use λ for the NORAD data base for λ^* in Eq. (18). To obtain the measurement time needed for any altitude or inclination range, just substitute the λ for that range in Eq. (18). Figure 7 gives the measurement time needed to achieve a given confidence that the estimate of the population of the NORAD data base is within 10, 20, 30, or 40%. Note that if the expected population is twice the NORAD population, the measurement time required to achieve the same confidence is half that given by Eq. (18) or in Fig. 7.

III. Algorithm Validation

To validate the algorithm we used the NORAD data base for March 26, 1991, and selected all of the objects with periods less than 2 h. Period (altitude) and inclination ranges were selected; and the number of objects in each bin is given in Table 2. Some of the objects in the NORAD data base have an RCS of −99 dBsm; these were changed to 0 dBsm.

The simulations for validation assumed a radar at Kwajalein, such as the GBR-X radar, which is located at a latitude of 10 deg. For the simulations a large radar beamwidth of 30 deg was used to reduce computation time. Increasing the beamwidth does not effect the results, it just decreases the computer time. These data are meant to be representative, except for the beamwidth. Since we had no detailed data on the GBR-X radar and many of the RCS values in the NORAD data base do not exist, we used a constant beamwidth in the simulations. The computer program propagates the orbits from the ephemerides in a space object data base, such as the NORAD data base, and determines the time and place in the beam for any object which penetrates a defined radar beam. The simulation time was based on sampling approximately 20% of the total population.

Figure 8 shows the estimated total number of objects for three simulations as a function of time (number of objects through the beam). The simulations differed only in the date and time at the beginning of the simulation. Note that there is

Table 2 NORAD population distribution

	Period							
Inclination, deg	87–95	95–100	100–105	105–110	110–115	115–120	120–140	Total
10.0–20.0	0	1	0	0	0	0	2	3
20.0–40.0	22	78	48	65	19	18	40	290
40.0–60.0	32	23	18	17	9	30	29	158
60.0–70.0	44	68	367	230	129	83	40	961
70.0–80.0	18	75	279	34	191	334	11	942
80.0–90.0	29	180	523	219	99	43	127	1220
90.0–100.0	57	201	461	183	76	4	19	1001
100.0–110.0	1	6	39	69	152	287	72	626
110.0–145.0	0	0	11	4	0	2	4	21
Total	203	632	1746	821	675	801	344	5222

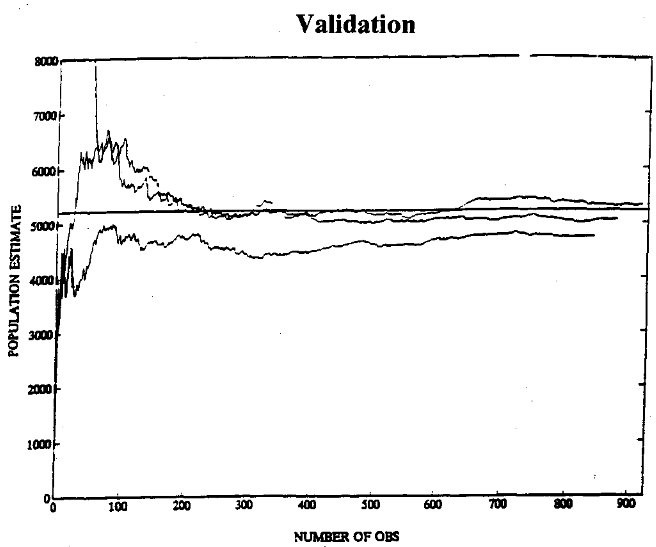

Fig. 8 Estimates of NORAD 51 population.

Table 3 Estimated population

	Sim 1	Sim 2	Sim 3
Estimated no. of objects	4736	5042	5325
Percent error	−9.3	−3.5	2.0
Actual no. of objects = 5222			
1σ = 3.3% or 174			

Table 4 Estimated period distribution

Period, min	Actual	Sim 1	Sim 2	Sim 3
87.0–95.0	203	157	225	298
95.0–100.0	632	641	714	830
100.0–105.0	1746	1479	1592	1779
105.0–110.0	821	750	788	709
110.0–115.0	675	554	484	479
115.0–120.0	801	750	819	746
120.0–240.0	344	406	420	483

Table 5 Estimated inclination distribution

Inclination, deg	Actual	Sim 1	Sim 2	Sim 3
10–20	3	4	2	4
20–40	290	270	265	292
40–60	158	126	131	143
60–70	961	774	924	1019
70–80	942	889	913	882
80–90	1220	1195	1053	1336
90–100	1001	820	1014	965
100–110	626	640	709	660
110–145	21	18	32	23

very little substantive change in the estimate after approximately 10% (500) of the objects have passed through the beam. Tables 3–5 and Figs. 9 and 10 show the estimated number of objects for the three simulations and the actual number for the period (altitude) and inclination ranges. These data show that the algorithm is valid; it does estimate the population and distribution of the low-orbit space objects.

IV. Error Sources

Errors in the estimate of the debris population and distribution can result from numerous sources which have been categorized as follows: 1) algorithmic, those errors which result from assumptions made in developing the algorithm; and 2) operational, those errors which arise from measurement errors and data processing. The effect of the major error sources in each of these categories is discussed subsequently.

Algorithmic Errors

Circular Orbit Assumption

For small eccentricities, i.e., to $\mathcal{O}(e)$, for half of the orbit the object will have a radius greater than the semimajor axis; and during the other half of the orbit it will be less than the semimajor axis. Thus, to $\mathcal{O}(e)$ the average altitude is the semimajor axis, and the effect of the circular orbit assumption has a negligible effect on the estimation of the total population. This is not true for the estimation of the altitude distribution. This can be demonstrated by examining a simplified example. Let the altitude range be divided into bins of equal altitude extent, let the population in each bin have a semimajor axis equal to the midpoint of the bin, and let the eccentricity distribution be the same in each bin. An altitude bin which has more objects than the two adjacent altitude bins will lose more objects than it gains. The error in the distribution estimation cannot be calculated because the eccentricity distribution is not known. For the NORAD data base, an estimate of the number of objects which would appear in the wrong bin can be calculated by simulation.

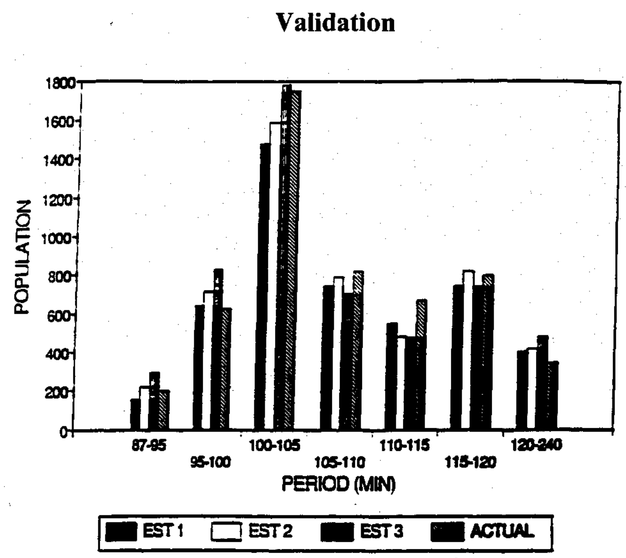

Fig. 9 NORAD 51 period distribution.

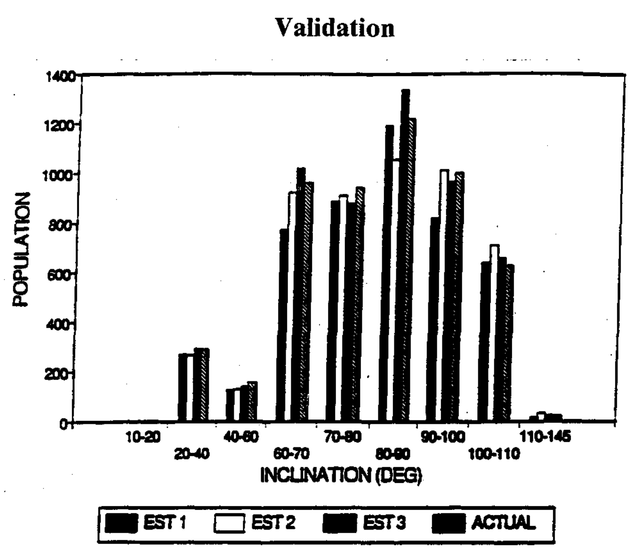

Fig. 10 NORAD 51 inclination distribution.

Right Ascension and Argument of Perigee Distribution

As stated in the Introduction, the uniform distribution assumption was validated by analysis of the NORAD data base. This means that all of the objects at the same altitude and inclination are equally probable to pass through the radar beam. Objects which have a repeatable ground track do not satisfy this property; their ground track either passes through the beam or it does not. However, orbit maintenance is required to maintain a repeatable ground track. Thus, a piece of debris will not have a repeatable ground track and any operational satellite which had such a repeatable ground track could be determined from the NORAD catalog. If this is considered to be a problem, the passage of any such satellite can be removed from the data. We do not consider this to be a problem.

Operational Errors

Altitude Measurement

If the altitude range measurements have no bias and the errors are typical of range measurements (<1 km), the effect on the estimation of the population and distribution is negligible.

Inclination Measurement

Inclination will be measured typically using monopulse. To estimate the effect of the inclination measurement error consider a space object population with all of the objects in circular orbits at the same altitude and inclination (I_0) and uniformly distributed in right ascension. Let the inclination measurement errors be uniformly distributed between ($I_0 - b$, $I_0 + b$). Then

$$E(\sin I) = \frac{1}{2b}\int_{-b}^{b} \sin(I_0 + x)\,dx \tag{19}$$

$$E(\sin I) = \sin I_0(\sin b/b) \tag{20}$$

$$E(\sin^2 I) = \frac{1}{2b}\int_{-b}^{b} \sin^2(I_0 + x)\,dx \tag{21}$$

$$E(\sin^2 I) = \sin^2 I_0 + \frac{\cos 2I_0}{2}\left[1 - \left(\frac{\sin 2b}{2b}\right)\right] \tag{22}$$

where E is the expectation operator.

As an example, let $I_0 = 60$ deg and $b = 10$ deg, that is, the inclination measurement is uniformly distributed in the range (50, 70). Equations (20) and (22) give

$$\mu_I = 59.5 \text{ deg} \tag{23}$$

$$\sigma_I = 0.167 \text{ deg} \tag{24}$$

The 0.5-deg error in the mean inclination causes less than 1% error in the population estimate. The 0.167-deg standard deviation shows that the additional error resulting from the spread of the inclination measurements will be small. Thus, relative large errors in the inclination measurement have a small effect on the population estimation. They will obviously have a larger effect on the inclination distribution.

Radar Side Lobes

Objects which are large enough to be detected when they pass through the side lobes will cause a problem if it is not determined they are in the side lobes and removed from the data. For those objects which are in the NORAD data base, this can be done by propagating the ephemeris and determining if they pass through the side lobes.

Radar Cross Section

Errors in the RCS measurement have no effect on the population estimate unless either the RCS or measured RCS is within 3 dB of the minimum detectable RCS. The effect on the population estimate is a function of the RCS distribution of objects and will have to be determined from simulation.

V. Conclusions

An algorithm is developed in this paper for estimating the low-Earth-orbit space object population and distribution in altitude, inclination, and radar cross section (RCS) from measurements obtained by a narrow beam vertical-looking radar which measures the range, inclination, and RCS of each object passing through the beam. Estimates of the error in the population and distribution as a function of the observation time are derived. The simulations showed that a good estimate of the population can be obtained with 10% of the objects passing through the beam. Effects of the fundamental assumptions and measurement errors on the estimation are discussed.

References

[1]Johnson, N. L., and Naver, D. S., "Orbital Debris Dedication: Techniques and Issues," AIAA Paper 90-1330, April 1990.

[2]McKay, D. S., "Microparticle Impact in Space: Results from Solar Max and Satellite and Shuttle Witness Inspections," NASA/Strategic Defense Initiative Organization (SDIO) Space Environmental Effects on Materials Workshop, NASA CP 3035, Pt. 1, 1989, pp. 301–316.

[3]Krasnekevich, J., Greeley, D. M., and Cunningham, P. M., "Use of GBR-X for Orbital Debris Radar," AIAA Paper 90-1352, April 1990.

[4]Stansbery, E. G., Bohannon, G., Pitts, C. C., Tracy, T., and Stanley, J. F., "Characterization of the Orbital Debris Environment Using the Haystack Radar," NASA Johnson Space Center, Rept. JSC-32213, Houston, TX, April 24, 1992.

[5]Papoulis, A., *Probability, Random Variables and Stochastic Processes,* McGraw-Hill, New York, 1984.

Alfred L. Vampola
Associate Editor